JOURNAL OF BACTERIOLOGY, Nov. 2004, p. 7680–7689 Vol. 186, No. 22
0021-9193/04/$08.00+0 DOI: 10.1128/JB.186.22.7680–7689.2004

A Novel Archaeal Alanine Dehydrogenase Homologous to Ornithine Cyclodeaminase and μ-Crystallin

Imke Schröder,[1]* Alexander Vadas,[2] Eric Johnson,[1] Sierin Lim,[2] and Harold G. Monbouquette[2]*

Department of Microbiology, Immunology and Molecular Genetics[1] and Department of Chemical Engineering,[2] University of California, Los Angeles, California

Received 6 May 2004/Accepted 16 August 2004

A novel alanine dehydrogenase (AlaDH) showing no significant amino acid sequence homology with previously known bacterial AlaDHs was purified to homogeneity from the soluble fraction of the hyperthermophilic archaeon *Archaeoglobus fulgidus*. AlaDH catalyzed the reversible, NAD^+-dependent deamination of L-alanine to pyruvate and NH_4^+. NADP(H) did not serve as a coenzyme. The enzyme is a homodimer of 35 kDa per subunit. The K_m values for L-alanine, NAD^+, pyruvate, NADH, and NH_4^+ were estimated at 0.71, 0.60, 0.16, 0.02, and 17.3 mM, respectively. The *A. fulgidus* enzyme exhibited its highest activity at about 82°C (203 U/mg for reductive amination of pyruvate) yet still retained 30% of its maximum activity at 25°C. The thermostability of *A. fulgidus* AlaDH was increased by more than 10-fold by 1.5 M KCl to a half-life of 55 h at 90°C. At 25°C in the presence of this salt solution, the enzyme was ~100% stable for more than 3 months. Closely related *A. fulgidus* AlaDH homologues were found in other archaea. On the basis of its amino acid sequence, *A. fulgidus* AlaDH is a member of the ornithine cyclodeaminase–μ-crystallin family of enzymes. Similar to the μ-crystallins, *A. fulgidus* AlaDH did not exhibit any ornithine cyclodeaminase activity. The recombinant human μ-crystallin was assayed for AlaDH activity, but no activity was detected. The novel *A. fulgidus* gene encoding AlaDH, AF1665, is designated *ala*.

Alanine dehydrogenase (AlaDH) catalyzes the reversible deamination of L-alanine to pyruvate (NAD^+ + L-alanine + $H_2O \leftrightarrow$ NADH + H^+ + pyruvate + NH_4^+).

The enzyme can serve both assimilatory and dissimilatory metabolic functions in various organisms. The characteristic NH_4^+ K_m value for AlaDH generally has been used as an arbitrary predictor of the assimilatory versus dissimilatory role of AlaDHs. AlaDHs from *Streptomyces fradiae* and pea and soybean bacteroids with relatively high affinities for ammonia (K_m, <10 mM) function primarily for NH_4^+ assimilation (3, 41, 49), while AlaDHs from other organisms have lower affinities for ammonia (K_m, >10 mM) and are therefore expected to act effectively in an assimilatory fashion only when high concentrations of NH_4^+ are present or when other pathways are repressed (6, 14, 29, 30, 35). In *Bacillus* sp., AlaDH has been implicated as the critical dissimilatory enzyme for generating pyruvate, the energy source for sporulation (39).

AlaDHs have been purified from a variety of bacteria and consist of a single catalytic subunit that, depending on the organism, assumes a homohexameric (11, 14, 23, 29, 30, 32, 35, 47), homotetrameric (5, 37, 41, 48), or homooctameric (49) quaternary complex. A comparison of the bacterial AlaDH amino acid sequences indicates that the enzyme is highly conserved, with ~50% sequence identity between individual AlaDHs (4). Significant sequence homology is also present between the bacterial AlaDHs and the alpha subunits and the N termini of bacterial and eukaryotic nicotinamide nucleotide transhydrogenase, respectively (4, 52). The AlaDH and pyridine nucleotide families of enzymes have glycine-rich regions in common that have been suggested to form a nucleotide-binding Rossman fold domain. Recently, the three-dimensional structure of the AlaDH from the cyanobacterium *Phormidium lapideum* was solved (4). Each AlaDH subunit of the hexameric enzyme consists of two compact domains that are separated by a cleft. The C terminus assumes a Rossman fold domain that binds NAD^+, and the substrate-binding site is located deep within the cleft and close to the binding site of the nicotinamide ring. Given the amino acid sequence similarity among the AlaDHs characterized to date, it can be expected that they will assume a similar tertiary structure.

Very little is known about archaeal AlaDHs. Two AlaDHs were purified or partially enriched from the halophilic archaea *Halobacterium salinarum* and *Halobacterium cutirubrum*, respectively (15, 17). Because the purification of these enzymes was performed about 20 years ago, no nucleotide sequence information for their genes is available. In addition, the *ald* gene encoding the bacterial-type AlaDH appears to be absent in the archaeal genomes that have been published thus far. The goals of this work were to establish whether AlaDH is also present in other archaea and to elucidate how it differs from the bacterial AlaDHs. With a native polyacrylamide gel electrophoresis (PAGE) activity staining procedure, AlaDH activity was detected in the hyperthermophilic archaeon *Archaeoglobus fulgidus*. *A. fulgidus* grows optimally at 83°C and uses sulfate reduction for energy generation (43, 44, 54). We describe here the purification and characterization of a novel archaeal AlaDH with no homology to known bacterial AlaDHs.

* Corresponding author. Mailing address for I.S.: Department of Microbiology, Immunology and Molecular Genetics, 1602 Molecular Sciences Bldg., Los Angeles, CA 90095-1489. Phone: (310) 825-8085. Fax: (310) 206-5231. E-mail: imkes@microbio.ucla.edu. Mailing address for H.G.M.: Chemical Engineering Department, 5531 Boelter Hall, University of California, Los Angeles, CA 90095. Phone: (310) 825-8946. Fax: (310) 206-4107. E-mail: hmonbouq@ucla.edu.

Homologues of the *A. fulgidus* enzyme are also present in other archaea, suggesting that the archaeal AlaDHs belong to a distinct evolutionary class of enzymes that is related to the μ-crystallin and ornithine cyclodeaminase (OCD) enzyme families.

MATERIALS AND METHODS

Organisms and growth conditions. *A. fulgidus* VC-16 (DSM 4304) served as the source of wild-type AlaDH and of the genomic DNA used in the PCR procedure to obtain the gene AF1665 encoding AlaDH. *A. fulgidus* was grown anaerobically on 10 mM sodium lactate and 30 mM sodium sulfate at 83°C, essentially as described by Zellner et al. (54) and modified as described by Vadas et al. (45). *A. fulgidus* biomass was produced in a 70-liter culture grown in a custom-built 100-liter glass-lined steel fermentor (Pfaudler, Rochester, N.Y.). The cells were harvested in the late log phase (~24 h after inoculation) at an optical density at 660 nm of 0.5 to 0.6 by concentration with an A/G Technology hollow-fiber unit (nominal molecular mass cutoff, 500 kDa) and subsequent centrifugation for 20 min at 16,000 × *g*. Cell yields were approximately 80 g (wet weight) per 70-liter culture. *Escherichia coli* strains DH5α (NEB) and BL21 (λDE3) (Stratagene) were used for plasmid maintenance and gene overexpression, respectively. For the culture of the *E. coli* strains, Luria-Bertani liquid and solid media containing ampicillin at a 100-mg/liter concentration were used.

Detection of AlaDH activity in native gels. The soluble fraction was prepared by a previously published high-pressure homogenization and centrifugation protocol (45) and separated by native PAGE with stacking and resolving gels of 4 and 8% polyacrylamide, respectively, with the Bio-Rad Mini-PROTEAN system. After electrophoresis, the gel was transferred to a 15-ml anaerobic culture tube sealed with a butyl rubber stopper to which the following anaerobic solutions were added: 5.0 ml of 100 mM Tricine buffer (pH 8.0), with 10 mM L-alanine, 0.05 mM phenazine methosulfate, 0.1 mg of methyl thiazolyl tetrazolium/ml, and 0.5 mM NAD^+. After incubation for 5 min at 85°C, AlaDH activity was identified as a dark purple formazan band in the gel (24).

Enzyme and protein assays. The protein concentration was measured by the Bradford assay (Bio-Rad) with bovine serum albumin as the standard. AlaDH activity was measured as oxidative deamination of alanine and as reductive amination of pyruvate by procedures adapted from previously described methods (28, 30). The assays were performed aerobically in stoppered quartz cuvettes at 82°C unless indicated otherwise. All assays were performed in triplicate, and the error range was within 6%. The oxidative deamination assay mixture contained 100 mM Tricine-KOH (pH 8.5) (titrated at 25°C), 5 mM L-alanine, and 2.5 mM NAD^+. The reductive amination assay mixture consisted of 100 mM Tricine-KOH (pH 8.5), 700 mM NH_4Cl, 5 mM pyruvic acid, and 0.08 mM NADH unless indicated otherwise. Rates were measured spectrophotometrically by following the reduction of NAD^+ for the deamination reaction or the oxidation of NADH for the amination reaction at 340 nm. One unit of activity is defined as 1 μmol NAD(H) reduced (or oxidized) per min. OCD activity was measured by a modified version of a previously published assay (33, 34). The reaction mixture, which contained 100 mM Tricine-KOH (pH 8.0) (titrated at 25°C), 10 mM ornithine, 1.0 mM NAD^+, and 0.3 μg of purified AlaDH, was incubated for 24 h at 37 or 80°C. The samples then were separated on cellulose K2F thin-layer chromatography plates (Whatman Ltd.) with 3:1 *n*-propanol–NH_3OH as the mobile phase. The presence of primary and secondary amines was detected with 0.2% ninhydrin dissolved in ethanol (10, 33). L-Proline and ornithine were used as standards.

Purification of AlaDH from *A. fulgidus*. All purification procedures were carried out aerobically at 25°C. The soluble fraction was prepared by a previously published high-pressure homogenization and centrifugation protocol (45). The soluble fraction (~400 mg of protein) was applied to a 5-ml Q Sepharose column (Pharmacia) equilibrated with 20 mM piperazine-*N*,*N*′-bis(2-ethanesulfonic acid) (PIPES)-NaOH (pH 7.0). After the column was washed with PIPES buffer containing 180 mM NaCl, AlaDH activity was eluted at 240 mM NaCl. The eluted protein was diluted with buffer to 100 mM NaCl and applied to a 5-ml Red Agarose 120 affinity column (Sigma) equilibrated with 20 mM PIPES-NaOH (pH 7.0)–100 mM NaCl. The column was washed with the equilibration buffer, and AlaDH was eluted with 350 mM NaCl in PIPES buffer. Ammonium sulfate was added to the eluted protein to a final concentration of 1.0 M. The solution was centrifuged and loaded onto a 1-ml Butyl Sepharose hydrophobic-interaction column (Pharmacia) equilibrated with PIPES buffer containing 1.0 M $(NH_4)_2SO_4$. The column was washed with 0.75 M $(NH_4)_2SO_4$, and AlaDH was eluted with 0.55 M $(NH_4)_2SO_4$ in PIPES buffer. The eluted protein was passed through a Centricon filter with a 100-kDa molecular mass cutoff (Amicon) and subsequently concentrated with a Centricon filter with a 30-kDa molecular mass cutoff. The concentrated protein was stored at −80°C.

SDS-gel electrophoresis. Proteins were separated on precast 20% homogeneous polyacrylamide gels under denaturing conditions with the Pharmacia PhastSystem. The protein samples were heated for 30 min at 100°C in 1% sodium dodecyl sulfate (SDS) prior to loading (24). The apparent molecular masses of the subunits of the purified AlaDH were estimated from the electrophoretic motility of the denatured protein. The molecular mass standards for SDS-PAGE were bovine albumin (66 kDa), chicken egg albumin (45 kDa), glyceraldehyde-3-posphate dehydrogenase (36 kDa), bovine carbonic anhydrase (29 kDa), bovine pancreas trypsinogen (24 kDa), soybean trypsin inhibitor (20 kDa), and bovine milk α-lactalbumin (14 kDa) (Sigma).

Native molecular weight determination. The native molecular weight of the AlaDH was determined with a Superose 6 (Pharmacia) gel filtration column. RNase A (13.7 kDa), chymotrypsinogen A (25 kDa), ovalbumin (43 kDa), and bovine serum albumin (67 kDa) were used as standards. The column was run with 20 mM PIPES buffer–300 mM NaCl (pH 7.0).

AlaDH pH and temperature optima. The pH optima for the AlaDH-catalyzed deamination and amination reactions were determined with the following buffers and pH values at 82°C: 100 mM morpholineethanesulfonic acid (MES) at pHs 6.1 and 6.15; 100 mM Tricine at pHs 6.5, 6.75, 6.8, 7.3, and 7.4; and 100 mM glycine at pHs 7.5, 7.9, 8.0, and 8.5. Temperature optima were determined at the indicated temperatures.

pH stability. The concentrated enzyme preparation was diluted 30-fold in the following buffers and pH values at 25°C: 100 mM glycine at pH 9.5, 100 mM Bicine at pH 9.0, 100 mM Tricine at pHs 8.5 and 8.0, 100 mM potassium phosphate at pHs 7.5 and 7.0, and 100 mM MES at pH 6.5. The samples were stored at 25°C in sterile microcentrifuge tubes, and the activity was monitored with the reductive amination assay over a period of 2 weeks.

Effect of salt on stability and activity. The desalted enzyme was concentrated with a centrifugal filter with a 30-kDa molecular mass cutoff (Amicon). Various salts [NaCl, KCl, $(NH_4)_2SO_4$, or K_2HPO_4] were added to the concentrated enzyme to give a final concentration of 1.0 M in PIPES buffer (pH 7.0). The samples were sealed in serum vials with butyl rubber stoppers and incubated at 90°C for 68 h. Periodically, samples were removed from the vials and AlaDH activity was measured with the reductive amination assay. The effect of the KCl concentration on enzyme activity was determined by adding 0.0, 0.5, 1.0, 1.5, and 2.0 M KCl to the reductive amination assay mixture.

Temperature-dependent stability. The AlaDH in 20 mM PIPES buffer (pH 7.0) (titrated at 25°C)–1.5 M KCl was incubated in stoppered serum vials at 25, 60, 90, and 100°C. The activity was monitored with the reductive amination assay on samples immediately after their removal from the vials.

N-terminal amino acid sequence analysis. The purified protein was run on an SDS–20% polyacrylamide gel and transferred to a Sequi-Blot polyvinylidene difluoride membrane (Bio-Rad). N-terminal amino acid sequence analysis was performed by the Protein Microsequencing Facility of the University of California, Los Angeles.

Phylogenetic analysis. Amino acid sequences homologous to the *A. fulgidus* AlaDH encoded by the AF1665 gene were identified with FASTA and BLASTp databases. The homologous amino acid sequences were aligned with Multialign (9). The amino acid alignment of selected proteins was displayed with GeneDoc (27). For database accession numbers, see the legend to Fig. 6. A phylogenetic tree was constructed with the neighbor-joining algorithm of TREECON (50). Evolutionary distances were calculated by Poisson correction with 1,000 bootstrap replicates.

Cloning and overexpression of *ala* and purification of recombinant AlaDH. Cloning and overexpression of *ala* and purification of recombinant AlaDH were done in parallel and in accordance with the protocol described by Smith et al. (42).

RESULTS

Detection of AlaDH activity in *A. fulgidus*. To examine the properties of an archaeal AlaDH, two archaeal representatives, *A. fulgidus* and *Pyrobaculum aerophilum*, were assayed spectrophotometrically for the reductive amination of pyruvate and for the oxidative deamination of alanine; however, no activity was detectable in either organism. Since both archaea had been cultured in the presence of yeast extract and peptone, it was possible that feedback inhibition by external amino acids resulted in very low AlaDH activity. To detect very low enzyme activity, a high-temperature, native PAGE activity assay was used. The advantage of such an approach is that low-abun-

TABLE 1. Purification of AlaDH from *A. fulgidus*

Prepn	Protein (mg)	Activity (U[a])	Recovery[c] (%)	Sp act (U/mg)	Purification (fold)
Soluble fraction	399	ND[b]	ND	ND	ND
Q Sepharose	48.3	17.2	100	0.3	1
Red agarose	0.8	16.7	97	22	62
Butyl Sepharose	0.4	10.4	60	25	70
100-kDa filter	0.04	7.3	43	203	572

[a] One unit is defined as the oxidation of 1 μmol of NADH per min in the reductive amination of pyruvate to L-alanine.
[b] ND, not detected.
[c] Recovery and fold purification assume that all of the AlaDH was recovered from the Q Sepharose step.

dance proteins are separated and assayed in situ, resulting in sensitive enzyme detection. Following electrophoreses, the gels were stained for oxidative deamination of alanine and concomitant reduction of NAD^+. The purple formazan band indicating AlaDH activity in *A. fulgidus* formed within 5 min at 85°C and was dependent on the presence of L-alanine in the assay buffer (data not shown). In contrast, no AlaDH activity could be detected in the soluble fraction of *P. aerophilum* (data not shown). AlaDH activity in the *A. fulgidus* soluble fraction was below the detection limit of the spectrophotometric assay used and could be measured only after enrichment of the enzyme.

Purification of AlaDH. The enzyme was purified to apparent homogeneity by Q Sepharose ion-exchange chromatography, Red Agarose 120 affinity chromatography, Butyl Sepharose hydrophobic interaction chromatography, and centrifugal filtration through a membrane with a 100-kDa cutoff (Table 1). After the final purification step, the enzyme was enriched 572-fold relative to the preparation obtained from the first chromatography column. Since AlaDH activity could not be quantified in the soluble fraction, recovery and fold purification were based on the AlaDH activity recovered from the Q Sepharose column. The purified AlaDH protein has an M_r of 35,000 as determined by SDS-PAGE. By size exclusion chromatography, the apparent molecular weight of the native protein was determined to be 76,000, suggesting that the enzyme is a homodimer (data not shown). The purified enzyme did not exhibit any significant absorption in the visible range, indicating that the enzyme does not contain chromophores such as flavins, Fe-S centers, or cytochromes.

Kinetic properties of AlaDH. After the final purification step, AlaDH catalyzed the oxidative deamination of alanine with a specific activity of 10.6 U/mg (k_{cat}, 6.1 s^{-1}) and the reductive amination of pyruvate with a specific activity of 203 U/mg (k_{cat}, 118 s^{-1}) (Table 2). The apparent affinity for pyruvate was fourfold higher than that for L-alanine (Table 2). The enzyme has an affinity for NH_4^+ that is in the same range as bacterial dissimilatory-type AlaDHs; however, the low abundance of AlaDH in *A. fulgidus* grown under rich-medium conditions argues against a dissimilatory function for this enzyme. An assimilatory function for *A. fulgidus* AlaDH is also supported by its low K_m for NADH. Its K_m for NAD^+ was more than an order of magnitude higher than that for NADH. *A. fulgidus* AlaDH is specific for NAD^+; $NADP^+$ was not used as a substrate. As is characteristic of many bacterial AlaDHs, the *A. fulgidus* enzyme exhibits substrate inhibition by pyruvate and NADH, but not by NAD^+ (Table 2) (2, 13, 29, 41).

TABLE 2. Kinetic properties of *A. fulgidus* AlaDH

Assay and substrate	k_{cat} (s^{-1})	K_m (mM)	k_{cat}/K_m (M^{-1} s^{-1}, 10^3)	K_i (mM)
Oxidative deamination[a]				
L-Alanine	6.1	0.71	9	16.8
L-2-Aminobutyrate	9.6	0.085	113	4.7
NAD^+	6.1	0.60	10	NI[b]
Reductive amination[a]				
Pyruvate	118	0.16	739	27.8
Ketobutyrate	143	0.48	298	4.8
Oxaloacetate	113	0.97	116	NI
NADH[d]	118	0.02	5,900	0.12
NH_4^+	118	17.3	7	ND[c]

[a] The assay was performed at pH 8.5 (titrated at 25°C) and 82°C.
[b] NI, no inhibition.
[c] ND, not determined.
[d] With pyruvate as the substrate.

Substrate specificity of AlaDH. A variety of L-amino acids and 2-oxo acids were tested as substrates for *A. fulgidus* AlaDH. In the deamination direction, only L-2-aminobutyrate is deaminated efficiently, at a rate about 1.5-fold higher than that determined for alanine (Tables 2 and 3). A ninefold lower K_m for L-2-aminobutyrate versus L-alanine suggests that L-2-aminobutyrate is the preferred substrate in the deamination reaction (Table 2). L-Valine, L-serine, L-threonine, L-aspartate, and L-isoleucine also served as substrates but at rates ≤12% of that for L-alanine (Table 3). Activity with several other natural amino acids was not detected. In the reductive amination direction, the enzyme exhibited high activity with 2-ketobutyrate and oxaloacetate compared to pyruvate (Tables 2 and 4). The Michaelis constants for 2-ketobutyrate and oxaloacetate were three- and sixfold larger, respectively, compared to the K_m for pyruvate (Table 2). Larger 2-keto acids of five and six carbons such as 2-ketovalerate and 2-ketocaproate were not suitable substrates (Table 4). The pyruvate derivatives 3-fluoropyruvate and 3-hydroxypyruvate resulted in lower activity compared to that obtained with pyruvate. The more bulky compound phenylpyruvate was not aminated reductively at a measurable rate.

pH and temperature optima of AlaDH. The pH optimum of AlaDH was ~7.0 for both the deamination and amination reactions (Fig. 1). AlaDH was not affected by prolonged incubation in buffers at the various pH values, indicating that the

TABLE 3. Substrate specificity for the oxidative deamination reaction of AlaDH

Substrate[a]	Sp act[c] (U/mg)
L-Alanine	10.6 ± 0.6
L-2-Aminobutyrate[b]	16.4 ± 1.0
L-Valine	1.30 ± 0.05
L-Serine	1.06 ± 0.05
L-Threonine	0.85 ± 0.05
L-Isoleucine	0.42 ± 0.02
L-Aspartate	0.42 ± 0.02
L-Lysine	<0.01
L-Tyrosine	<0.01
L-Proline	<0.01
L-Tryptophan	<0.01
L-Phenylalanine	<0.01

[a] Substrate concentration, 5 mM.
[b] L-2-Aminobutyrate concentration, 1 mM.
[c] The assays were performed at pH 8.5 (titrated at 25°C) and 82°C.

TABLE 4. Substrate specificity of the reductive amination reaction of AlaDH

Substrate (concn, mM)	Sp act[a] (U/mg)
Pyruvate (5)	203 ± 12
3-Fluoropyruvate (5)	40.6 ± 2.4
Hydroxypyruvate (5)	20.3 ± 1.2
Oxaloacetate (1)	195 ± 12
Ketobutyrate (1)	246 ± 15
Ketovalerate (10)	12.2 ± 0.7
Ketocaproate (10)	4.1 ± 0.2
Phenylpyruvate (10)	<0.1

[a] The assays were performed at pH 8.5 (titrated at 25°C) and 82°C.

observed pH optimum is a reflection of the protonation and deprotonation of active site amino acid residues. The temperature optimum was approximately 82°C as measured for the reductive amination of pyruvate assay (Fig. 2). This temperature optimum correlates well with the optimum growth temperature of *A. fulgidus* (83°C) (54). It is noteworthy that 30% of the activity remained at 25°C.

Effects of salt on AlaDH temperature stability. When incubated at 90°C for 2 h, AlaDH lost its activity completely (Fig. 3). However, the addition of various salts at a 1.0 M concentration increased stability at 90°C by more than an order of magnitude (Fig. 3). Of these, KCl proved to be optimal for stabilizing enzyme activity. The optimum KCl concentration for stability was determined to be 1.5 M (Fig. 4). In 1.5 M KCl, the enzyme half-life at 90°C was extended to 55 h (Fig. 5). At 25°C, no loss of activity could be detected for more than 3 months in the presence of 1.5 M KCl. AlaDH activity was not measurably affected by the addition of up to 2.0 M KCl to the enzyme assay.

N-terminal amino acid sequence analysis of AlaDH. The N-terminal sequence of *A. fulgidus* AlaDH was determined to be Met-Glu-Thr-Leu-Ile-Leu-Thr-Gln-Glu-Glu-Val-Glu-Ser-Leu. This sequence corresponds to the translated AF1665 gene locus in the *A. fulgidus* genome (19). The protein predicted by AF1665 consists of 323 amino acids and has a calculated molecular weight of 34,828, which is consistent with the value estimated for the purified AlaDH protein by SDS-PAGE. The theoretical pI of the protein is 5.18.

OCD activity. The gene locus AF1665 had been annotated to encode an OCD. OCD catalyzes the conversion of ornithine to proline in the catabolism of opines, which are synthesized in crown gall tumors of plants infected by *Agrobacterium tumefa-*

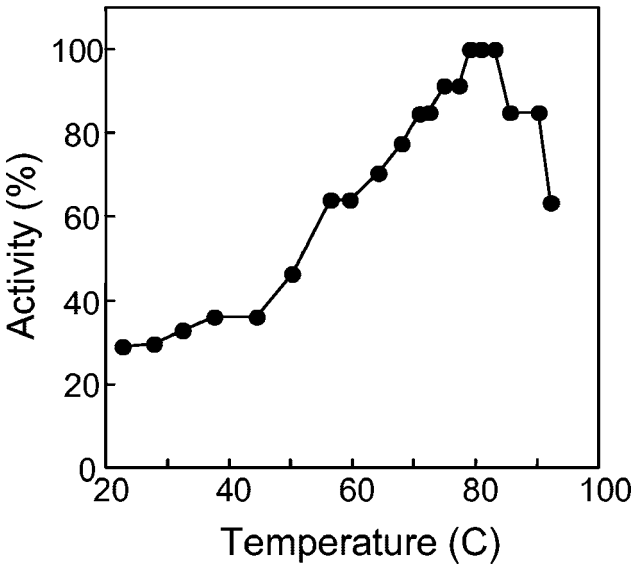

FIG. 2. Temperature dependence of *A. fulgidus* AlaDH activity. One hundred percent activity corresponds to 203 U/mg.

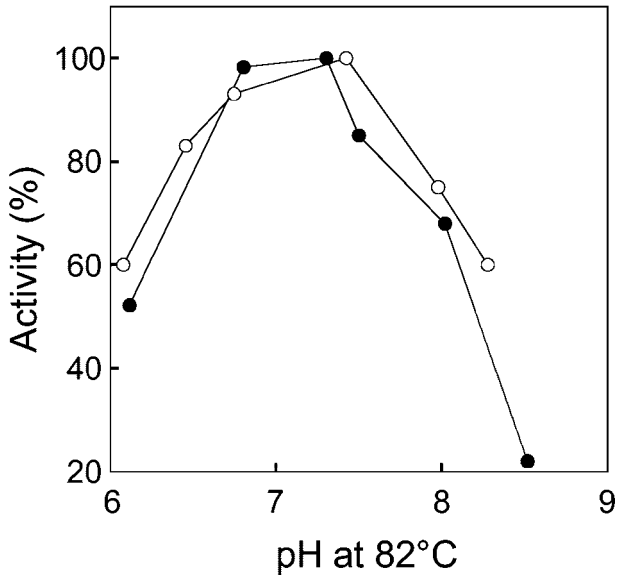

FIG. 1. pH dependence of *A. fulgidus* AlaDH activity for oxidative deamination (filled circles) and reductive amination (open circles). One hundred percent activity corresponds to 203 U/mg.

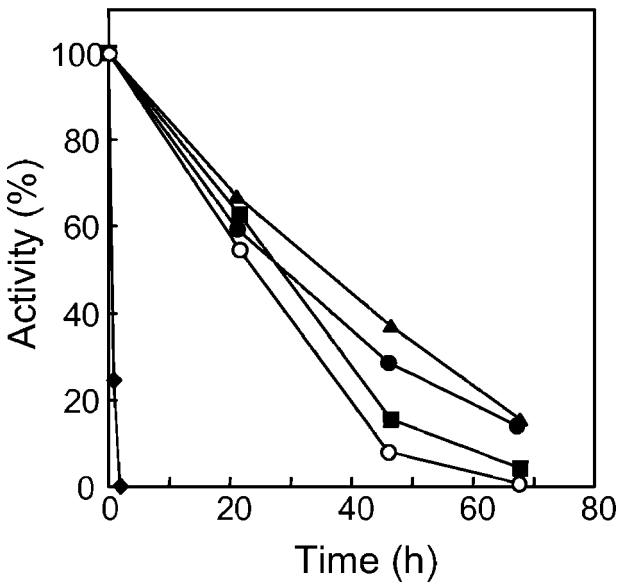

FIG. 3. Effect of salt on the temperature stability of *A. fulgidus* AlaDH. The enzyme was incubated at 90°C in the presence of no added salt (filled diamonds), 1.0 M KCl (filled triangles), 1.0 M NaCl (filled circles), 1.0 M $(NH_4)_2SO_4$ (filled squares), or 1.0 M K_2HPO_4 (open circles). One hundred percent activity corresponds to 203 U/mg.

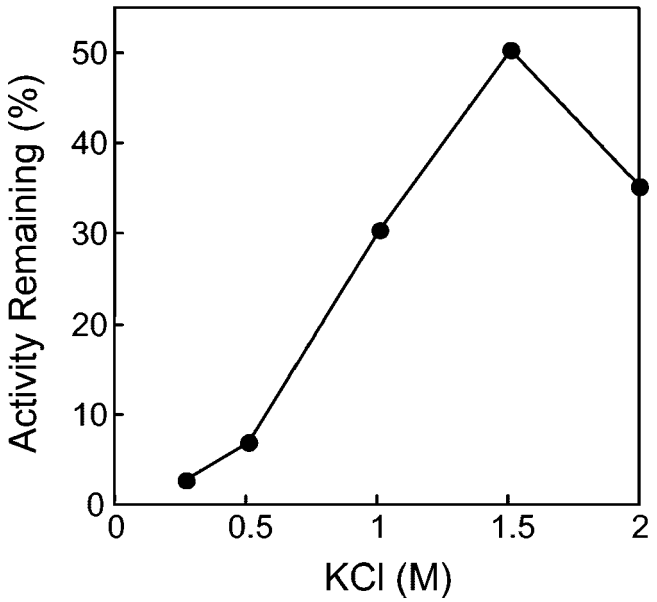

FIG. 4. Activity of *A. fulgidus* AlaDH after 55 h at 90°C as a function of KCl concentration. One hundred percent activity corresponds to 203 U/mg.

ciens (7, 33, 36). To test whether AlaDH also exhibited OCD activity, the purified enzyme was incubated with ornithine at 80 and 37°C; however, no proline was detected (data not shown). This suggests that *A. fulgidus* AlaDH is not an OCD. The detection limit of the method was approximately 1% of the activity measured for L-alanine deamination.

Expression of *ala* and characterization of the recombinant enzyme. To confirm that the AF1665 gene locus encodes AlaDH, the AF1665 gene was cloned from the *A. fulgidus* chromosome into an *E. coli* overexpression vector (42). After induction of gene expression in *E. coli*, a 35-kDa protein was produced. The activity of the recombinant protein in the *E. coli* soluble cell fraction was barely detectable, i.e., <0.05 U/mg, but increased to 113 U/mg after incubation for 20 min at 80°C, suggesting that the enzyme requires an elevated temperature to assume an active conformation. Recombinant *A. fulgidus* AlaDH was purified to homogeneity, and the measured kinetic and stability properties of the recombinant AlaDH protein were indistinguishable from those of the native enzyme (data not shown).

Analysis of primary structure and phylogenetic relationships. FASTA and BLASTP searches with the *A. fulgidus* AlaDH amino acid sequence revealed homologous proteins, which were aligned with ClustalW (Fig. 6). No apparent homology to any bacterial AlaDHs was identified, suggesting that *A. fulgidus* AlaDH constitutes an independent class of enzymes. The AF1665 gene is now designated *ala* to distinguish it from the *ald* genes encoding bacterial AlaDHs.

A. fulgidus AlaDH is 31 to 34% identical to the family of OCD enzymes in *A. tumefaciens*. It is also about 33 to 35% identical to the mammalian μ-crystallin family that includes the human thyroid hormone-binding protein (THBP) (51). μ-Crystallins are structural proteins present in the eye lenses of marsupials and are found in various tissues in other organisms, including humans, where their function is uncertain (18, 38, 53). Other homologous proteins (about 27% identity) include the lysine cyclodeaminase from *Streptomyces hygroscopicus* (16), an enzyme that is more closely related to the OCD family, and several hypothetical proteins from various bacteria and archaea. The proteins most closely related to *A. fulgidus* AlaDH are encoded by open reading frames from other archaea, the hyperthermophile *Methanothermobacter thermoautotrophicum* and the mesophile *Halobacterium* sp. strain NCR-1, with 49 and 46% sequence identity, respectively, which supports a prediction that these proteins will prove to be AlaDHs.

Visual inspection of the aligned amino acid sequences revealed highly conserved residues (Fig. 6). Among these, a GxGxxA/S motif (Gly132, Gly134, and Ala137 in the *A. fulgidus* sequence), suggesting a NAD^+ binding site, is located in the central part of the proteins. While the glycine residues are conserved in the entire family of enzymes, Gly/Ala is not conserved completely.

On the basis of the sequence alignment, a phylogenetic tree was constructed (Fig. 7). The tree branches into 10 major groups with long lineages, indicating the functional diversity of the proteins. Because of the long lineages, it was difficult to assign an unambiguous relationship of each group to another. Therefore, the tree is shown in a collapsed form, in which the relationship of the groups to one another is not taken into consideration. Three of the groups contain proteins with a known function. They include group I with the subgroup of μ-crystallin proteins, group V with OCDs and lysine cyclodeaminases (RapL of *S. hygroscopicus*), and group X containing *A. fulgidus* AlaDH. While nine groups appear to consist of proteins with functions that are predicted to be identical or very similar, group I contains proteins from very diverse organisms such as mammals, insects, yeast, plants, bacteria, and a strikingly large number of hyperthermophilic archaea. Whether proteins in this group have the same or diverse activities has yet to be established.

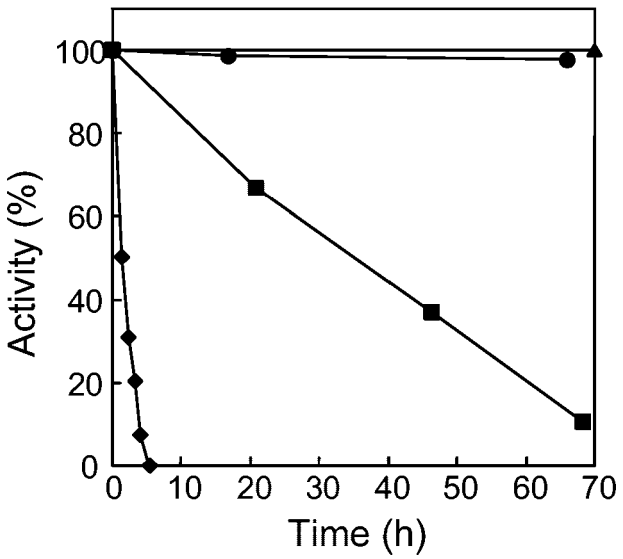

FIG. 5. Temperature stability of *A. fulgidus* AlaDH. The enzyme was incubated with 1.5 M KCl at ambient temperature (triangles), 60°C (circles), 90°C (squares), or 100°C (diamonds). One hundred percent activity corresponds to 203 U/mg.

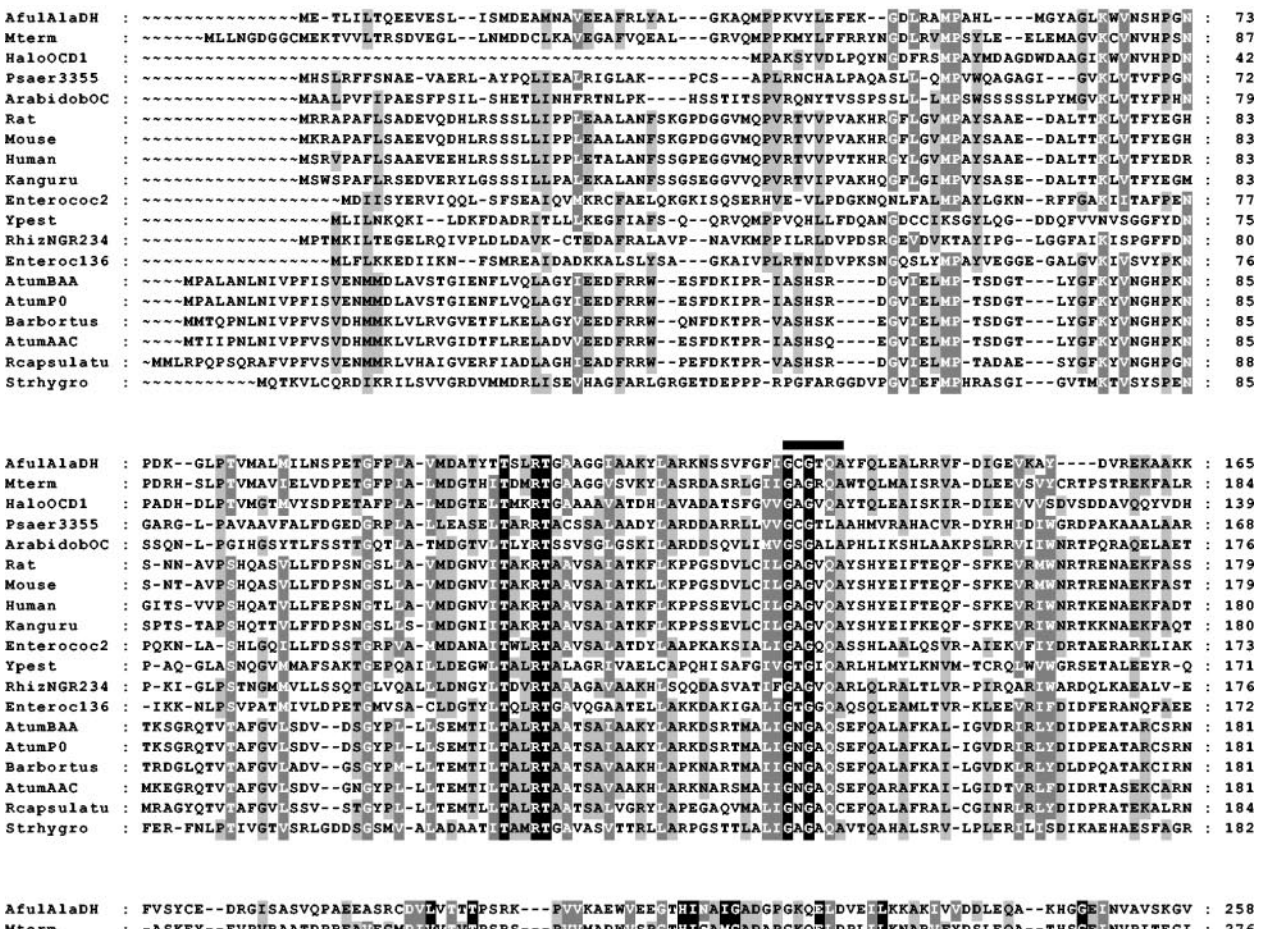

FIG. 6. Comparison of the amino acid sequence of *A. fulgidus* AlaDH to those of selected homologues. For accession numbers, see the legend to Fig. 7. The thick line denotes the proposed NAD-binding site. The aligned C-terminal 23 amino acid residues of *A. fulgidus* AlaDH are not shown since the alignment did not reveal any significant conservation.

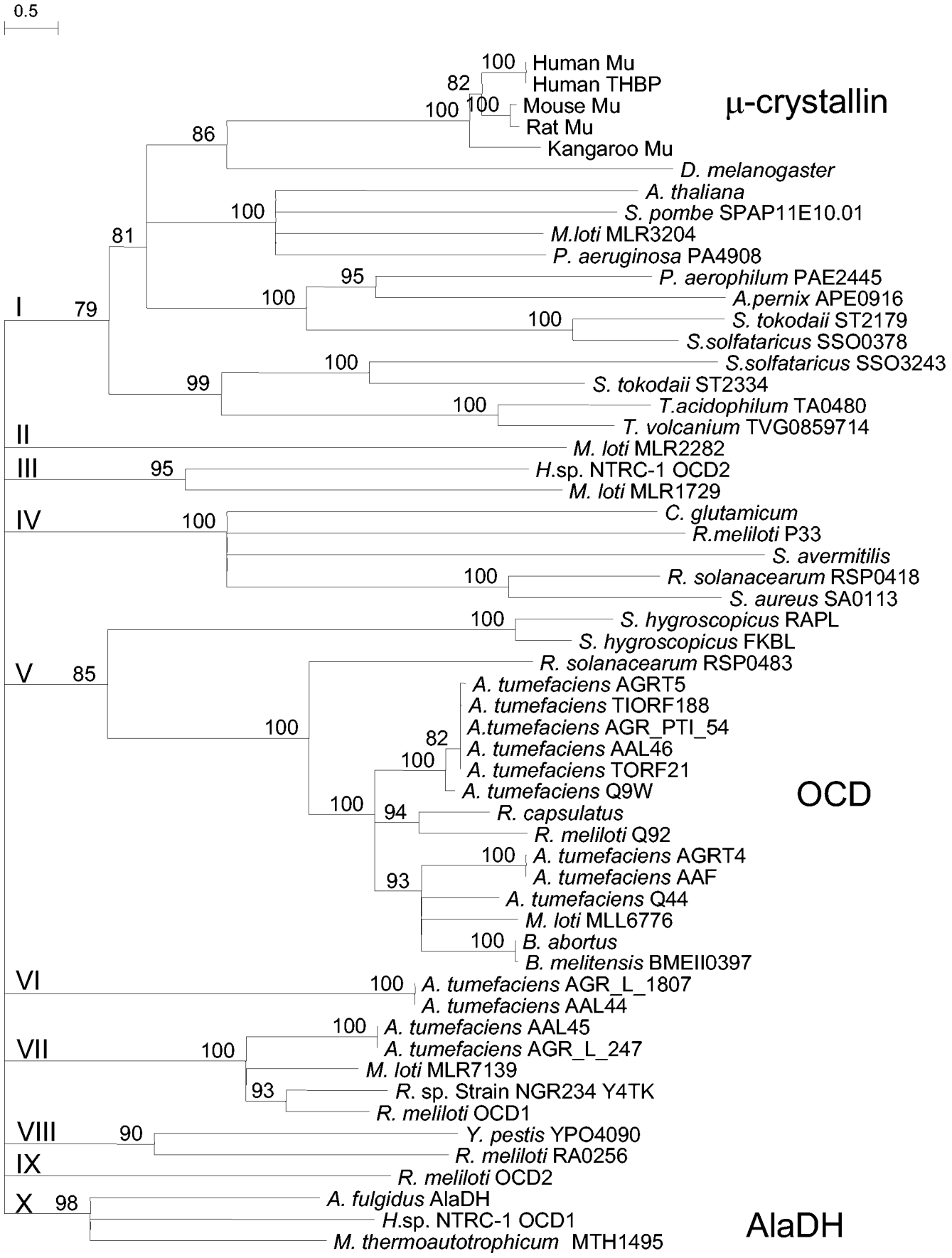
0.5
Human Mu
Human THBP
Mouse Mu
Rat Mu
Kangaroo Mu
μ-crystallin
D. melanogaster
A. thaliana
S. pombe SPAP11E10.01
M.loti MLR3204
P. aeruginosa PA4908
P. aerophilum PAE2445
A.pernix APE0916
S. tokodaii ST2179
S.solfataricus SSO0378
S.solfataricus SSO3243
S. tokodaii ST2334
T.acidophilum TA0480
T. volcanium TVG0859714
M. loti MLR2282
H.sp. NTRC-1 OCD2
M. loti MLR1729
C. glutamicum
R.meliloti P33
S. avermitilis
R. solanacearum RSP0418
S. aureus SA0113
S. hygroscopicus RAPL
S. hygroscopicus FKBL
R. solanacearum RSP0483
A. tumefaciens AGRT5
A. tumefaciens TIORF188
A.tumefaciens AGR_PTI_54
A. tumefaciens AAL46
A. tumefaciens TORF21
A. tumefaciens Q9W
OCD
R. capsulatus
R. meliloti Q92
A. tumefaciens AGRT4
A. tumefaciens AAF
A. tumefaciens Q44
M. loti MLL6776
B. abortus
B. melitensis BMEII0397
A. tumefaciens AGR_L_1807
A. tumefaciens AAL44
A. tumefaciens AAL45
A. tumefaciens AGR_L_247
M. loti MLR7139
R. sp. Strain NGR234 Y4TK
R. meliloti OCD1
Y. pestis YPO4090
R. meliloti RA0256
R. meliloti OCD2
A. fulgidus AlaDH
H.sp. NTRC-1 OCD1
M. thermoautotrophicum MTH1495
AlaDH
I
II
III
IV
V
VI
VII
VIII
IX
X

Assay of human μ-crystallin for AlaDH activity. Many eye lens proteins exhibit enzyme activity, such as ε-crystallin, which was shown to have lactate dehydrogenase activity (53). To establish whether the human μ-crystallin exhibits AlaDH activity, purified recombinant human μ-crystallin was generously provided by G. Wistow (National Institutes of Health) and assayed for reversible AlaDH activity at 37°C; however, no activity was detected.

DISCUSSION

We report here the characterization of a novel, extremely thermostable AlaDH protein that shows no significant sequence homology to previously known AlaDHs. The *A. fulgidus* enzyme exhibits kinetics similar to those of AlaDHs from bacteria, albeit at a far higher temperature of 82°C, which is consistent with the optimal growth temperature for *A. fulgidus* (54). Previously described AlaDHs from thermophilic bacteria show remarkable thermal stability, yet the *A. fulgidus* enzyme is extraordinary by comparison. For example, the AlaDHs of *Bacillus sphaericus* and *Thermus thermophilus* exhibit half-lives of ~70 and ~10 min at 80 and 85°C, respectively (29, 47), whereas the *A. fulgidus* enzyme has a half-life of 50 min at 90°C at low ionic strength and ~55 h at 90°C in 1.5 M KCl (Fig. 3 and 5). KCl is one of the known osmolytes in marine archaea and has been suggested to serve as a general stabilizer for proteins (21, 31). It is particularly noteworthy that this enzyme retains 30% of its maximal activity at 25°C. *A. fulgidus* AlaDH therefore represents a striking counterexample to the widely held generalization that extremely thermostable enzymes from hyperthermophiles should be expected to show very little or no activity at or near 25°C (20). Because of its high stability and activity at 25°C, *A. fulgidus* AlaDH lends itself to the in vitro synthesis of L-alanine (46).

Consistent with most of the characterized bacterial AlaDHs, the reductive amination of pyruvate to L-alanine is catalyzed by the archaeal enzyme at a higher maximum rate in vitro than is the deamination of L-alanine (14, 28–30, 32, 35, 37). However, enzymes with K_m values above 10 mM may not be very effective for assimilation since intracellular ammonium concentrations usually do not exceed 10 mM. Experimentally determined k_{cat}/K_m values provide for a better comparison of AlaDH efficiency in the oxidative and reductive directions, yet the k_{cat}/K_m values compiled to date do not show a strong correlation with the physiological function of bacterial AlaDHs deduced from gene regulation experiments. *A. fulgidus* AlaDH exhibits similar catalytic efficiencies in both directions ($k_{cat}/K_{m,Ala} = 9 \times 10^3\ M^{-1}\ s^{-1}$; $k_{cat}/K_{m,NH_4^+} = 7 \times 10^3\ M^{-1}\ s^{-1}$; Table 2). It is therefore not possible to discern the physiological role of AlaDH on the basis of its kinetic properties. *A. fulgidus* also contains a very abundant $NADP^+$-dependent glutamate dehydrogenase with an ammonium K_m of 4 mM that could serve as the primary nitrogen assimilatory enzyme (1). It is not known whether the *ala* gene is regulated in *A. fulgidus*; however, studies to elucidate the physiological role of this enzyme are under way.

The AlaDH protein from *A. fulgidus* is selective for L-alanine and L-2-aminobutyrate in the oxidative direction, although 12% or lower activity is also obtained with other L-amino acids such as valine, serine, threonine, isoleucine, and aspartate. Minor deamination activities of other L-amino acids (about 5% of the activity with L-alanine) are common features of many bacterial AlaDHs, although enzymes with high substrate specificity also exist (8, 23, 28, 30, 47, 49). However, *A. fulgidus* AlaDH distinguishes itself by its unusually high L-2-aminobutyrate deamination activity. Substrate specificity for the other known archaeal AlaDHs from *H. salinarum* and *H. cutirubrum* were not determined (15, 17).

Recently, an L-2-aminobutyrate dehydrogenase was purified from the archaeon *Halobacterium saccharovorum* (25). The *H. saccharovorum* L-2-aminobutyrate dehydrogenase also deaminates L-alanine, but at a twofold slower rate. The K_m values for L-2-aminobutyrate and L-alanine are similar to those of *A. fulgidus* AlaDH. The subunit molecular weight of the *H. saccharovorum* L-2-aminobutyrate dehydrogenase (M_r, 54,000) is larger than that of *A. fulgidus* AlaDH, and it assumes a tetrameric quaternary structure while *A. fulgidus* AlaDH constitutes a dimer. Although the amino acid sequence of the *H. saccharovorum* L-2-aminobutyrate dehydrogenase is not known, it is possible that this enzyme is related to *A. fulgidus* AlaDH. As is typical for enzymes from halophiles, the *H. saccharovorum* L-2-aminobutyrate dehydrogenase is only stable in the presence of high salt concentrations.

FIG. 7. Condensed phylogenetic tree of the archaeal AlaDH–OCD–μ-crystallin family. The values at the internodes are bootstrap values. The Roman numerals indicate the 10 subfamilies. The letter coding behind each genus name indicates the gene locus or protein, where available. In some cases the beginning of the accession number was used to differentiate paralogues. The organisms, in alphabetical order with the accession numbers in parentheses, are *Aeropyrum pernix* APE0916 (Q9YDJ7), *A. tumefaciens* AGR_L_247 (AAK88692), *A. tumefaciens* AAF (AAF77139), *A. tumefaciens* AAL44 (AAL44751), *A. tumefaciens* AAL45 (AAL45552), *A. tumefaciens* AAL46 (AAL46252), *A. tumefaciens* Q44 (Q44332), *A. tumefaciens* Q9W (Q9WWA2), *A. tumefaciens* AGR_L_1807 (AAK89477), *A. tumefaciens* AGR_PTI_54 (AAK90974), *A. tumefaciens* AGRT4 (Q59701), *A. tumefaciens* AGRT5 (P09773), *A. tumefaciens* TIORF188 (Q9R693), *A. tumefaciens* TORF21 (Q9R468), *Arabidopsis thaliana* (Q9FLY0), *A. fulgidus* AlaDH AF1665 (O28608), *Brucella abortus* (Q59175), *Brucella melitensis* BMEII0397 (Q8YCY1), *Corynebacterium glutamicum* (Q9Z468), *Drosophila melanogaster* CG4872 (AAL68180), *Halobacterium* sp. strain NRC-1 OCD1 (Q9HN71), *Halobacterium* sp. strain NRC-1 OCD2 (Q9HQ24), *Homo sapiens* Mu (AAH18061), *H. sapiens* THBP (Q14894), *Macropus fuliginosus* Mu (Q28488), *Mesorhizobium loti* MLL6776 (Q988E2), *M. loti* MLR1729 (Q98JY2), *M. loti* MLR2282 (Q98IR6R), *M. loti* MLR3204 (Q98GR8), *M. loti* MLR7139 (Q987A2), *Methanothermobacter thermautotrophicum* MTH1495 (027539), *Mus musculus* Mu (O54983), *Pseudomonas aeruginosa* PA4908 (Q9HUQ5), *P. aerophilum* PAE2445 (Q8ZV60), *Ralstonia solanacearum* RSP0418 (Q8XSP9), *R. solanacearum* RSP0483 (Q8XSJ1), *Rattus norvegicus* Mu (Q9QYU4), *Rhizobium meliloti* P33 (P33728), *R. meliloti* Q92 (Q92U20), *R. meliloti* OCD1 (P58338), *R. meliloti* OCD2 (P58339), *R. meliloti* RA0256 (Q930E2), *Rhizobium* sp. strain NGR234 Y4TK (P55665), *R. capsulatus* (O68052), *Schizosaccharomyces pombe* SPAP11E10.01 (Q9HDZ0), *Staphylococcus aureus* SA0113 (Q99X98), *Streptomyces avermitilis* (Q93H28), *S. hygroscopicus* var. *ascomyceticus* FKBL (Q9KIE2), *S. hygroscopicus* RAPL lysine cyclodeaminase (Q54304), *Sulfolobus solfataricus* SSO0378 (Q980D6), *S. solfataricus* SSO3243 (Q97TY8), *S. tokodaii* ST2179 (Q96YJ3), *S. tokodaii* ST2334 (Q96Y33), *Thermoplasma acidophilum* TA0480 (Q9HKW3), *T. volcanium* TVG0859714 (Q97AH2), and *Yersinia pestis* YPO4090 (Q8Z9V2).

It is possible that archaeal AlaDHs function as an AlaDH and as an L-2-aminobutyrate dehydrogenase. While 2-ketobutyrate is a common pathway intermediate, L-2-aminobutyrate is a so-called "unnatural" amino acid that can be formed when 2-ketobutyrate accumulates. High levels of 2-ketobutyrate have been shown to be toxic to *Salmonella enterica* serovar Typhimurium (22). Therefore, amination of 2-ketobutyrate to the less inhibitory compound L-2-aminobutyrate may serve as a detoxification mechanism.

In the reductive amination direction, *A. fulgidus* AlaDH exhibits a broader substrate range, which appears to be a feature common to many AlaDHs (14, 17, 28, 30, 49). 2-Ketobutyrate, oxaloacetate, and pyruvate are aminated at similar rates (Tables 2 and 4). However, a comparison of the catalytic efficiencies indicates that pyruvate is the preferred substrate for reductive amination. It is noteworthy that *A. fulgidus* AlaDH also acts as a reversible serine dehydrogenase, since it both aminates hydroxypyruvate to L-serine and deaminates L-serine, but at 10% of the rates obtained with pyruvate and alanine (Tables 3 and 4).

Strikingly, *A. fulgidus* AlaDH has no significant amino acid sequence similarity to previously described bacterial AlaDHs and thus belongs to an independent class of enzymes. Instead, *A. fulgidus* AlaDH exhibits homology to bacterial OCD and the mammalian μ-crystallin family of proteins (Fig. 6 and 7). The highest sequence similarity, however, exists to proteins from two archaea, *M. thermoautotrophicum* and *Halobacterium* sp. strain NRC-1, suggesting that these proteins may function as AlaDHs and not as OCDs as they have been annotated (26, 40). There is no amino acid sequence information available for the *H. salinarum* and *H. cutirubrum* AlaDH enzymes (15, 17). Interestingly, Graupner and White detected OCD activity in cell extracts of the hyperthermophilic methanogen *Methanococcus jannaschii* (12). This archaeon lacks any AlaDH or OCD homologue, suggesting that proline formation from ornithine is catalyzed by a novel, not yet characterized, enzyme.

Recently, the three-dimensional structure of the AlaDH enzyme from the cyanobacterium *P. lapideum* was solved (4). On the basis of the analysis of this structure, *P. lapideum* AlaDH belongs to a family of D-2-hydroxy acid dehydrogenases that also includes D-lactate dehydrogenases, D-glycerate dehydrogenase, D-phosphoglycerate dehydrogenase, NAD^+-dependent formate dehydrogenase, and D-2-hydroxyisocaproate dehydrogenase (4). Despite the structural similarity, there is no significant sequence similarity in this enzyme family, with the exception of an NAD^+ binding site, i.e., the common dinucleotide-binding fingerprint, GxGxxA/G (4). This motif is present as GxGxxA/S in *A. fulgidus* AlaDH and homologues, with the notable exception of the putative OCD from *Rhodobacter capsulatus*, where the motif is GxGxxC (Fig. 6).

Smith et al. recently solved the three-dimensional structure of *A. fulgidus* AlaDH, and a detailed description of this structure will follow (42). The crystal structure confirmed the dimeric quaternary structure of *A. fulgidus* AlaDH, demonstrating that each monomer consists of two domains, a Rossman fold domain for NAD^+ binding and a catalytic domain that is, however, structurally unrelated to the catalytic domain of *P. lapideum* AlaDH (11a).

The different primary and tertiary structures of bacterial and archaeal AlaDHs suggest that these enzymes did not evolve from a common ancestor but that evolution occurred along two separate pathways. Since *A. fulgidus* AlaDH homologues are present in all three domains of life, archaea, bacteria, and eucarya, it is likely that this type of enzyme was present in the last common ancestor. Alternatively, an early horizontal gene transfer event among the three domains could have occurred. After the divergence of the bacteria, archaea, and eucarya, the predecessor protein appears to have evolved into a diverse group of proteins with specialized functions. Thus, *A. fulgidus* AlaDH does not exhibit OCD activity and the human μ-crystallin protein lacks both OCD and AlaDH activities. Whether any of the OCDs have AlaDH activity is not known.

Interestingly, the μ-crystallin group of this diverse enzyme family includes several closely related archaeal homologues (group I in Fig. 7). The μ-crystallin proteins and the related protein THBP are found in human and animal eye lens retinas and in diverse tissues that respond to thyroid hormone regulation, including human, kangaroo, and rat brain, heart, skeletal muscle, and kidney tissues, respectively (18, 38). Neither the human μ-crystallin nor the *P. aerophilum* μ-crystallin homologue exhibits any detectable AlaDH activity, assuming that the latter protein is expressed. Elucidation of the function of the archaeal μ-crystallin homologues may aid in understanding the physiology of the human and animal μ-crystallins.

In conclusion, *A. fulgidus* AlaDH is a representative of a new archaeal line of AlaDHs that is distinct from the bacterial AlaDHs. We predict that once more archaeal genomes become available, the number of archaeal AlaDHs in group X will increase (Fig. 7).

ACKNOWLEDGMENTS

We thank Graeme Wistow (National Institutes of Health) for the generous gift of recombinant human μ-crystallin. Funding for H.G.M. was provided by U.S. Department of Commerce-National Institute of Standards and Technology cooperative agreement 70NANB7H0009. I.S. was supported by the National Science Foundation (MCB-0091351). E.J. was supported by U.S. Public Health Service National Research Service award GM07185.

REFERENCES

1. **Aalen, N., I. Steen, N. Birkeland, and T. Lien.** 1997. Purification and properties of an extremely thermostable $NADP^+$-specific glutamate dehydrogenase from *Archaeoglobus fulgidus*. Arch. Microbiol. **168:**536–539.
2. **Aharonowitz, Y., and C. G. Friedrich.** 1980. Alanine dehydrogenase of the β-lactam producer *Streptomyces clavuligerus*. Arch. Microbiol. **125:**137–142.
3. **Allaway, D., E. M. Lodwig, L. A. Crompton, M. Wood, R. Parsons, T. R. Wheeler, and P. S. Poole.** 2000. Identification of alanine dehydrogenase and its role in mixed secretion of ammonium and alanine by pea bacteroids. Mol. Microbiol. **36:**508–515.
4. **Baker, P. J., Y. Sawa, H. Shibata, S. E. Sedelnikova, and D. W. Rice.** 1998. Analysis of the structure and substrate binding of *Phormidium lapideum* alanine dehydrogenase. Nat. Struct. Biol. **5:**561–567.
5. **Bellion, E., and F. Tan.** 1987. An NAD^+-dependent alanine dehydrogenase from a methylotrophic bacterium. Biochem. J. **244:**565–570.
6. **Caballero, F. J., J. Cardenas, and F. Castillo.** 1989. Purification and properties of L-alanine dehydrogenase of the phototrophic bacterium *Rhodobacter capsulatus* E1F1. J. Bacteriol. **171:**3205–3210.
7. **Cho, K. Y., C. Fuqua, B. S. Martin, and S. C. Winans.** 1996. Identification of *Agrobacterium tumefaciens* genes that direct the complete catabolism of octopine. J. Bacteriol. **178:**1872–1880.
8. **Chowdhury, E. K., T. Saitoh, S. Nagata, M. Ashiuchi, and H. Misono.** 1998. Alanine dehydrogenase from *Enterobacter aerogenes*: purification, characterization, and primary structure. Biosci. Biotechnol. Biochem. **62:**2357–2363.
9. **Corpet, F.** 1988. Multiple sequence alignment with hierarchical clustering. Nucleic Acids Res. **16:**10881–10890.
10. **Dessaux, Y., A. Petit, J. Tempé, M. Demarez, C. Legrain, and J.-M. Wiame.** 1986. Arginine catabolism in *Agrobacterium* strains: role of the Ti plasmid. J. Bacteriol. **166:**44–50.
11. **Galkin, A., L. Kulakova, H. Ashida, Y. Sawa, and N. Esaki.** 1999. Cold-

adapted alanine dehydrogenases from two Antarctic bacterial strains: gene cloning, protein characterization, and comparison with mesophilic and thermophilic counterparts. Appl. Environ. Microbiol. **65:**4014–4020.

11a. **Gallagher, D. T., H. G. Monbouquette, I. Schröder, H. Robinson, M. J. Holden, and N. N. Smith.** 2004. Structure of archaeal alanine dehydrogenase and relation to bacterial and human proteins. J. Mol. Biol. **342:**119–130.

12. **Graupner, M., and R. H. White.** 2001. *Methanococcus jannaschii* generates L-proline by cyclization of L-ornithine. J. Bacteriol. **183:**5203–5205.

13. **Grimshaw, C. E., and W. W. Cleland.** 1981. Kinetic mechanism of *Bacillus subtilis* L-alanine dehydrogenase. Biochemistry **20:**5650–5655.

14. **Hutter, B., and M. Singh.** 1999. Properties of the 40 kDa antigen of *Mycobacterium tuberculosis*, a functional L-alanine dehydrogenase. Biochem. J. **343:**669–672.

15. **Keradjopoulos, D., and A. W. Holldorf.** 1979. Purification and properties of alanine dehydrogenase from *Halobacterium salinarium*. Biochim. Biophys. Acta **570:**1–10.

16. **Khaw, L. E., G. A. Bohm, S. Metcalfe, J. Staunton, and P. F. Leadlay.** 1998. Mutational biosynthesis of novel rapamycins by a strain of *Streptomyces hygroscopicus* NRRL 5491 disrupted in *rapL*, encoding a putative lysine cyclodeaminase. J. Bacteriol. **180:**809–814.

17. **Kim, E. K. and P. S. Fitt.** 1977. Partial purification and properties of *Halobacterium cutirubrum* L-alanine dehydrogenase. Biochem. J. **161:**313–320.

18. **Kim, R. Y., R. Gasser, and G. J. Wistow.** 1992. Mu-crystallin is a mammalian homologue of *Agrobacterium*-ornithine cyclodeaminase and is expressed in human retina. Proc. Natl. Acad. Sci. USA **89:**9292–9296.

19. **Klenk, H. P., R. A. Clayton, J. F. Tomb, O. White, K. E. Nelson, K. A. Ketchum, R. J. Dodson, M. Gwinn, E. K. Hickey, J. D. Peterson, D. L. Richardson, A. R. Kerlavage, D. E. Graham, N. C. Kyrpides, R. D. Fleischmann, J. Quackenbush, N. H. Lee, G. G. Sutton, S. Gill, E. F. Kirkness, B. A. Dougherty, K. McKenney, M. D. Adams, B. Loftus, S. Peterson, C. I. Reich, L. K. McNeil, J. H. Badger, A. Glodek, L. Zhou, R. Overbeek, J. D. Gocayne, J. F. Weidman, L. McDonald, T. Utterback, M. D. Cotton, T. Spriggs, P. Artiach, B. P. Kaine, S. M. Sykes, P. W. Sadow, K. P. D'Andrea, C. Bowman, C. Fujii, S. A. Garland, T. M Mason, G. J. Olsen, C. M. Fraser, H. O. Smith, C. R. Woese, and J. C. Venter.** 1997. The complete genome sequence of the hyperthermophilic, sulphate-reducing archaeon *Archaeoglobus fulgidus*. Nature **390:**364–370.

20. **Kohen, A., R. Cannio, S. Bartolucci, and J. P. Klinman.** 1999. Enzyme dynamics and hydrogen tunneling in a thermophilic alcohol dehydrogenase. Nature **399:**496–499.

21. **Lamosa, P., D. L. Turner, R. Ventura, C. Maycock, and H. Santos.** 2003. Protein stabilization by compatible solutes. Effect of diglycerol phosphate on the dynamics of *Desulfovibrio gigas* rubredoxin studied by NMR. Eur. J. Biochem. **270:**4606–4614.

22. **LaRossa, R. A., T. K. Van Dyk, and D. R. Smulski.** 1987. Toxic accumulation of α-ketobutyrate caused by inhibition of the branched-chain amino acid biosynthetic enzyme acetolactate synthase in *Salmonella typhimurium*. J. Bacteriol. **169:**1372–1378.

23. **Laue, H., and A. M. Cook.** 2000. Purification, properties and primary structure of alanine dehydrogenase involved in taurine metabolism in the anaerobe *Bilophila wadsworthia*. Arch. Microbiol. **174:**162–167.

24. **Manchenko, G.** 1994. A handbook of detection of enzymes on electrophoretic gels. CRC Press, Inc., Boca Raton, Fla.

25. **Nagata, S., Y. Kobayashi, S. Shinkawa, R. Katoh, T. Ohshima, and H. Misono.** 2003. Novel halophilic 2-aminobutyrate dehydrogenase from *Halobacterium saccharovorum* DSM 1137. J. Mol. Catal. B Enzym. **23:**223–230.

26. **Ng, W. V., S. P. Kennedy, G. G. Mahairas, B. Berquist, M. Pan, H. D. Shukla, S. R. Lasky, N. S. Baliga, V. Thorsson, J. Sbrogna, S. Swartzell, D. Weir, J. Hall, T. A. Dahl, R. Welti, Y. A. Goo, B. Leithauser, K. Keller, R. Cruz, M. J. Danson, D. W. Hough, D. G. Maddocks, P. E. Jablonski, M. P. Krebs, C. M. Angevine, H. Dale, T. A. Isenbarger, R. F. Peck, M. Pohlschroder, J. L. Spudich, K. H. Jung, M. Alam, T. Freitas, S. B. Hou, C. J. Daniels, P. P. Dennis, A. D. Omer, H. Ebhardt, T. M. Lowe, R. Liang, M. Riley, L. Hood, and S. DasSarma.** 2000. Genome sequence of *Halobacterium* species NRC-1. Proc. Natl. Acad. Sci. USA **97:**12176–12181.

27. **Nicholas, K. B., H. B. Nicholas, Jr., and D. W. Deerfield II.** 1997. GeneDoc: analysis and visualization of genetic variation. EMBNEW News **4:**14.

28. **Ohshima, T., and K. Soda.** 1979. Purification and properties of alanine dehydrogenase from *Bacillus sphaericus*. Eur. J. Biochem. **100:**29–39.

29. **Ohshima, T., M. Sakane, T. Yamazaki, and K. Soda.** 1990. Thermostable alanine dehydrogenase from thermophilic *Bacillus sphaericus* DSM 462—purification, characterization and kinetic mechanism. Eur. J. Biochem. **191:**715–720.

30. **Porumb, H., D. Vancea, L. Muresan, E. Presecan, I. Lascu, I. Petrescu, T. Porumb, R. Pop, and O. Barzu.** 1987. Structural and catalytical properties of L-alanine dehydrogenase from *Bacillus cereus*. J. Biol. Chem. **262:**4610–4615.

31. **Roberts, M. F.** 2000. Osmoadaptation and osmoregulation in archaea. Front. Biosci. **5:**796–812.

32. **Rowell, P., and W. D. P. Stewart.** 1976. Alanine dehydrogenase of the N_2-fixing blue-green alga, *Anabaena cylindrica*. Arch. Microbiol. **107:**115–124.

33. **Sans, N., U. Schindler, and J. Schröder.** 1988. Ornithine cyclodeaminase from Ti plasmid C58: DNA sequence, enzyme properties and regulation of activity by arginine. Eur. J. Biochem. **173:**123–130.

34. **Sans, N., G. Schröder, and J. Schröder.** 1987. The Noc region of Ti plasmid C58 codes for arginine and ornithine cyclodeaminase. Eur. J. Biochem. **167:**81–87.

35. **Sawa, Y., M. Tani, K. Murata, H. Shibata, and H. Ochiai.** 1994. Purification and characterization of alanine dehydrogenase from a cyanobacterium, *Phormidium lapideum*. J. Biochem. **116:**995–1000.

36. **Schindler, U., N. Sans, and J. Schröder.** 1989. Ornithine cyclodeaminase from octopine Ti plasmid Ach5: identification, DNA sequence, enzyme properties, and comparison with gene and enzyme from nopaline Ti plasmid C58. J. Bacteriol. **171:**847–854.

37. **Schuffenhauer, G., T. Schrader, and J. R. Andreesen.** 1999. Morpholine-induced formation of L-alanine dehydrogenase activity in *Mycobacterium* strain HE5. Arch. Microbiol. **171:**417–423.

38. **Segovia, L., J. Horwitz, R. Gasser, and G. Wistow.** 1997. Two roles for mu-crystallin: a lens structural protein in diurnal marsupials and a possible enzyme in mammalian retinas. Mol. Vis. **3:**9.

39. **Siranosian, K. J., K. Ireton, and A. D. Grossman.** 1993. Alanine dehydrogenase (Ald) is required for normal sporulation in *Bacillus subtilis*. J. Bacteriol. **175:**6789–6796.

40. **Smith, D. R., L. A. Doucette-Stamm, C. Deloughery, H. Lee, J. Dubois, T. Aldredge, R. Bashirzadeh, D. Blakely, R. Cook, K. Gilbert, D. Harrison, L. Hoang, P. Keagle, W. Lumm, B. Pothier, D. Qiu, R. Spadafora, R. Vicaire, Y. Wang, J. Wierzbowski, R. Gibson, N. Jiwani, A. Caruso, D. Bush, H. Safer, D. Patwell, S. Prabhakar, S. McDougall, G. Shimer, A. Goyal, S. Pietrokovski, G. M. Church, C. J. Daniels, J. Mao, P. Rice, J. Nölling, and J. N. Reeve.** 1997. Complete genome sequence of *Methanobacterium thermoautotrophicum* ΔH: functional analysis and comparative genomics. J. Bacteriol. **179:**7135–7155.

41. **Smith, M. T., and D. W. Emerich.** 1993. Alanine dehydrogenase from soybean nodule bacteroids—kinetic mechanism and pH studies. J. Biol. Chem. **268:**10746–10753.

42. **Smith, N., M. Mayhew, H. Robinson, A. Heroux, D. Charlton, M. J. Holden, and D. T. Gallagher.** 2003. Crystallization and phasing of alanine dehydrogenase from *Archaeoglobus fulgidus*. Acta Crystallogr. D Biol. Crystallogr. **59:**2328–2331.

43. **Stetter, K. O.** 1988. *Archaeoglobus fulgidus* gen. nov., sp. nov.: a novel taxon of extremely thermophilic archaebacteria. Syst. Appl. Microbiol. **10:**172–173.

44. **Stetter, K. O., G. Lauerer, M. Thomm, and A. Neuner.** 1987. Isolation of extremely thermophilic sulfate reducers: evidence of a novel branch of archaebacteria. Science **236:**822–824.

45. **Vadas, A., H. G. Monbouquette, and I. Schröder.** 1999. Identification and characterization of a novel ferric reductase from the hyperthermophilic archaeon *Archaeoglobus fulgidus*. J. Biol. Chem. **274:**36715–36721.

46. **Vadas, A. J., I. Schröder, and H. G. Monbouquette.** 2002. Room-temperature synthesis of L-alanine using the alanine dehydrogenase of the hyperthermophilic archaeon *Archaeoglobus fulgidus*. Biotechnol. Prog. **18:**909–911.

47. **Váli, Z., F. Kilár, S. Lakatos, S. A. Venyaminov, and P. Závodszky.** 1980. L-Alanine dehydrogenase from *Thermus thermophilus*. Biochim. Biophys. Acta **615:**34–47.

48. **Vancura, A., I. Vancurová, J. Volc, S. K. T. Jones, M. Flieger, G. Basarová, and V. Behal.** 1989. Alanine dehydrogenase from *Streptomyces fradiae*. Eur. J. Biochem. **179:**221–227.

49. **Vancurová, I., A. Vancura, J. Volc, J. Neuzil, M. Flieger, G. Basarová, and V. Behal.** 1988. Purification and partial characterization of alanine dehydrogenase from *Streptomyces aureofaciens*. Arch. Microbiol. **150:**438–440.

50. **Van de Peer, Y., and R. De Wachter.** 1994. TREECON for Windows: a software package for the construction and drawing of evolutionary trees for the Microsoft Windows environment. Comput. Appl. Biosci. **10:**569–570.

51. **Vie, M. P., C. Evrard, J. Osty, A. BretonGilet, P. Blanchet, M. Pomerance, P. Rouget, J. Francon, and J. P. Blondeau.** 1997. Purification, molecular cloning, and functional expression of the human nicodinamide-adenine dinucleotide phosphate-regulated thyroid hormone-binding protein. Mol. Endocrinol. **11:**1728–1736.

52. **Williams, R., N. P. J. Cotton, C. M. Thomas, and J. B. Jackson.** 1994. Cloning and sequencing of the genes for the proton-translocating nicotinamide nucleotide transhydrogenase from *Rhodospirillum rubrum* and the implications for the domain structure of the enzyme. Microbiology **140:**1595–1604.

53. **Wistow, G., and H. Kim.** 1991. Lens protein expression in mammals—taxon-specificity and the recruitment of crystallins. J. Mol. Evol. **32:**262–269.

54. **Zellner, G., E. Stackebrandt, H. Kneifel, P. Messner, U. B. Sleytr, E. C. De Marcario, H.-P. Zabel, K. O. Stetter, and J. Winter.** 1989. Isolation and characterization of a thermophilic, sulfate reducing Archaebacterium, Archaeoglobus fulgidus strain Z. Syst. Appl. Microbiol. **11:**151–160.